

## BREAKUP OF LIQUID THREADS IN LINEAR FLOWS

D. V. KHAKHAR and J. M. OTTINO

Department of Chemical Engineering, Goessmann Laboratory, University of Massachusetts, Amherst,  
MA 01003, U.S.A.

(Received 15 September 1985; in revised form 20 May 1986)

**Abstract**—We study, theoretically, the surface-tension-driven breakup of a long filament of fluid in a general linear flow,  $v = L \cdot x$ . By analyzing the problem in a moving frame and assuming a circular cross section we find that the flow around the filament is an axisymmetric extensional flow with a time-dependent strength, which can be calculated from the rate of rotation of the filament and a contribution to the axial velocity which varies with the azimuthal angle. The analysis of the axisymmetric time-dependent case does not appear to be overly restrictive: the asymmetric variation may be small even in the case of a simple shear flow, in which the asymmetry is the greatest among all possible linear flows, depending on the initial orientation of the filament. We present calculations for two special cases: hyperbolic extensional flow and simple shear flow. The results indicate that under similar conditions, the drop fragments produced on breakup in simple shear flow are larger than those in hyperbolic extensional flow. The predictions of the theory also compare reasonably well with some previous experimental data in hyperbolic extensional flow and simple shear flow.

### INTRODUCTION

The instability of filaments of fluid with regard to surface disturbances has been the subject of a number of experimental and theoretical studies. Such analyses are of relevance to the study of the mixing and dispersion of immiscible liquids in which drops may be stretched into filaments prior to breakup.

It has been demonstrated by several experimental studies in two-dimensional flows (Taylor 1934; Karam & Bellinger 1968; Grace 1971; Torza *et al.* 1972; Bentley 1985) that the strain rate of the flow around the drop must exceed a critical strain rate to break it into smaller fragments. In the case of creeping flow around the drop the critical strain rate is dependent mainly on the ratio of the viscosity of the drop to that of the suspending fluid and the type of flow (simple shear, hyperbolic extensional flow etc.). Theoretical analyses have been reasonably successful in predicting the critical strain rate for linear flows [see the review paper by Rallison (1984)], the usual criterion for breakup being the non-existence of stable drop shapes beyond the critical strain rate. Here our aim is to gain an understanding of the breakup process itself by considering the surface-tension-driven breakup of a filament of fluid acted upon by a linear flow.

The breakup of an extending cylindrical thread of fluid as a model for an elongated drop was first analyzed theoretically by Tomotika (1936), who worked on the problem based on a suggestion of Taylor. The flow far from the drop was taken to be an axisymmetric extensional flow and the drop was assumed to be infinitely long. The analysis yielded a complex non-linear ordinary differential equation describing the growth of axisymmetric sinusoidal disturbances on the surface of the drop. An asymptotic analysis for long times showed that although the disturbances were damped by the flow initially, at later times they were sufficiently magnified to cause breakup. Several years later, and using the same assumptions, Mikami *et al.* (1975) presented an improved version of the analysis of Tomotika (1936) and carried out a thorough numerical analysis of the system to obtain the drop size and initial amplitude of the disturbance as a function of the time for breakup for a fixed strain rate and viscosity ratio. They also obtained asymptotic estimates for a number of quantities, and carried out experiments to study the breakup of drops in a two-dimensional extensional flow. Comparison of the theory with the experiments was justified by showing that the cross section of the drop would become circular for sufficiently slender drops. The experimental values for the dimensionless wavenumber at breakup, taken for two viscosity ratios and a number of different strain rates, agreed reasonably well with the theoretical predictions for an average strain rate, the results being relatively insensitive to changes in strain rate. The

dynamics of drop breakup were also investigated experimentally by Grace (1971). The time for breakup, the length of the drop at breakup and the number of drops produced on breakup were recorded for a drop in a simple shear flow for a fixed viscosity ratio and a number of values of strain rate exceeding the critical strain rate. The number of fragments produced on breakup increased dramatically with increasing strain rate and the dimensionless time for breakup decreased. The main effect of the external strain rate was to damp out disturbances on the surface of the drop, thus postponing the breakup until the drop was more elongated. Experiments with a programmed strain rate, in which the drop was extended to its critical deformation and then the strain rate reduced to keep the deformation constant, showed that breakup occurred sooner in this case.

It is clear from the analyses described above that the external flow has a significant impact on the dynamics of the breakup of drops. In practice the flow encountered by a drop in a mixer is complex and the analysis of breakup seems to be intractable due to the complications introduced by non-symmetric drop shapes, the unknown velocity field around the drop etc. Here we restrict ourselves to the simpler case of an infinitely long cylindrical drop in the linear flow

$$\mathbf{v}^\infty = \mathbf{L} \cdot \mathbf{x}$$

with the assumption that the drop cross section remains circular due to its slenderness. Such a problem, especially with  $\mathbf{L}$  as a function of time, is relevant to the local description of mixing of immiscible fluids (Khakhar *et al.* 1984).

In general, in such a flow, there is a tendency of the drop cross section to become non-circular. When the drop is sufficiently elongated, however, surface tension acts to restore the cross section to a circular shape [see Mikami *et al.* (1975)]. Here we assume that the drop is sufficiently slender so that the cross section is nearly circular. We realize the latter condition by omitting terms in the imposed flow which tend to make the cross section non-circular, in a manner similar to that used by Hinch & Acrivos (1980) in their analysis of a slender, pointed drop in a simple shear flow.

### A FLUID FILAMENT IN A LINEAR FLOW

We consider the stretching and rotation of an infinitely long fluid filament of viscosity  $\mu_i$  suspended in a fluid of viscosity  $\mu_e$ , with the viscosity ratio,  $p$ , defined as  $p = \mu_i/\mu_e$ . The flow far from the drop is

$$\bar{\mathbf{v}}^\infty = \bar{\mathbf{L}} \cdot \bar{\mathbf{x}}$$

and the Reynolds number with respect to the filament radius is vanishingly small. The velocity field with respect to a moving frame with the second-order harmonic terms omitted is then

$$\begin{aligned} v_z^\infty &= G_1 z + (g_{12} \cos \phi + g_{13} \sin \phi) r, \\ v_r^\infty &= -G_1 r/2 + (g_{21} \cos \phi + g_{31} \sin \phi) z, \\ v_\phi^\infty &= (g_{31} \cos \phi - g_{21} \sin \phi) z + (g_{32} - g_{23}) r/2, \end{aligned}$$

where

$$g_{ij} = \dot{Q}_{ip} Q_{jp} + (1 - \delta_{ij}) Q_{ip} \bar{L}_{pq} Q_{jq}$$

and

$$G_i = \mathbf{D} : \mathbf{e}_i \mathbf{e}_i \quad (\text{no sum on } i).$$

The vector  $\mathbf{e}_i$  is a unit vector in the coordinate direction  $i$  and  $\mathbf{D}$  is the stretching tensor with respect to the moving frame.  $\mathbf{Q}$  is an orthogonal matrix specifying the rotation of the frame and is to be found from the analysis. A vector is represented in the two frames by

$$\mathbf{x} = \mathbf{Q} \cdot \bar{\mathbf{x}},$$

where the overbar refers to quantities with respect to the fixed frame.

Assuming creeping flow around the drop, the equations for the flow are

$$\left. \begin{aligned} \mu_m \nabla^2 \mathbf{u}_m &= \nabla P_m \\ \nabla \cdot \mathbf{u}_m &= 0 \end{aligned} \right\} \quad m = i, e,$$

where the subscripts  $i$  and  $e$  refer to the internal and external flow, respectively. The boundary conditions to be satisfied by the flow are

$$\begin{aligned} \mathbf{u}_e &= \mathbf{v}^\infty, & r &\rightarrow \infty, \\ \mathbf{u}_e &= \mathbf{u}_i, & r &= a, \\ T_{rz}^e &= T_{rz}^i, & r &= a, \end{aligned}$$

and

$$T_{rr}^e - T_{rr}^i = \frac{\sigma}{a}, \quad r = a,$$

for all  $z$ , where  $a$  is the radius of the filament,  $\sigma$  is the surface tension and  $\mathbf{T}^m$  is the stress tensor. In the above equations  $\mathbf{v}^\infty$  refers to the simplified velocity field in which the second-order harmonics of  $\phi$  are neglected. A velocity field which satisfies the equations is

$$\begin{aligned} u_{ze} &= G_1 z + r \left[ 1 + \frac{a^2(1-p)}{r^2(1+p)} \right] (g_{12} \cos \phi + g_{13} \sin \phi), \\ u_{re} &= -\frac{G_1 r}{2}, \\ u_{\phi e} &= 0 \end{aligned}$$

outside the filament, and

$$\begin{aligned} u_{zi} &= G_1 z + \frac{2}{(1+p)} (g_{12} \cos \phi + g_{13} \sin \phi) r, \\ u_{ri} &= -\frac{G_1 r}{2}, \\ u_{\phi i} &= 0 \end{aligned}$$

inside the filament, provided that the filament rotates according to the following two conditions:

$$g_{23} = g_{32}$$

and

$$g_{21} = g_{31} = 0.$$

The condition  $g_{23} = g_{32}$  specifies a solid-body rotation about the drop axis which does not contribute to the breakup in any way. The conditions  $g_{21} = g_{31} = 0$  specify the rotation in the two normal directions,  $\mathbf{e}_2$  and  $\mathbf{e}_3$ . Substituting  $\bar{\mathbf{m}} = \mathbf{Q}^T \cdot \mathbf{e}_1$  in the expressions for  $g_{21}$  and  $g_{31}$  and simplifying we find

$$\bar{\mathbf{m}} = \mathbf{L}\bar{\mathbf{m}} - (\mathbf{D} : \bar{\mathbf{m}}\bar{\mathbf{m}})\bar{\mathbf{m}},$$

where  $\bar{\mathbf{m}}$  is a unit vector oriented along the drop axis with respect to the fixed frame. From the normal stress boundary condition we obtain

$$(P_i + \mu_i G_1) - (P_e + \mu_e G_1) = \frac{\sigma}{a},$$

where  $P_i$  and  $P_e$  are the constant pressures inside and outside the filament, respectively.

The above analysis indicates that the velocity field with respect to a frame rotating with the drop is essentially an axisymmetric extensional flow with a non-axisymmetric shear flow along its surface.

In addition it indicates that the drop rotates and stretches as a material element in the flow. The above results are confirmed by an analysis of the stretching of pointed drops when the length of the drop tends to infinity (Hinch & Acrivos 1980; Khakhar & Ottino 1986). In the case of drops of a finite length in flows which are not purely extensional, however, there is a tendency of the drop axis to bend (Hinch & Acrivos 1980) which we neglect in our analysis. The approximation improves as the imposed flow becomes more extensional in character and as the drop length increases.

### GROWTH OF SURFACE DISTURBANCES ON THE FLUID THREAD

When the deformation of the filament due to the surface instability is small, the velocity field is only slightly perturbed from the undisturbed flow found earlier and can be separated as

$$v_m^i = u_m + \epsilon v_m^*, \quad m = i, e,$$

where  $\epsilon v_m^*$  is the flow generated by the instability. The asterisk denotes quantities pertaining to the disturbance flow, the small parameter  $\epsilon$  is related to the amplitude of the disturbance and the superscript  $t$  pertains to the total or resulting flow. The disturbance flow must also satisfy the creeping flow equations separately.

The drop shape is given by

$$R = a + \epsilon f(z, \phi),$$

where  $\epsilon f(z, \phi)$  is the small varicosity of the drop surface caused by the disturbance flow. In the case of an axisymmetric extensional flow, Tomotika (1936) showed that small amplitude axisymmetric disturbances are sinusoidal with

$$f(z) = \alpha \cos(kz),$$

where  $\alpha$  is the amplitude and  $k$  the wavenumber. In the case of a general linear flow, however, disturbances which are initially axisymmetric will be convected by the flow along the drop surface, resulting in a non-symmetric drop (figure 1b). Here we consider the case when the asymmetry is small and the varicosity is given by

$$f(z, \phi) = \alpha \cos(kz + \epsilon_1 k a \beta), \quad [1]$$

where  $\beta = \beta(\phi)$  specifies the non-axisymmetric phase shift of the disturbance caused by the surface flow and  $\epsilon_1$  is a small parameter specifying the deviation from symmetry which we assume to be of the same order of magnitude as  $\epsilon$ . Physically, the case of small asymmetry considered above corresponds to the situation when the distance that a disturbance is convected during its growth is small in comparison to its wavelength.

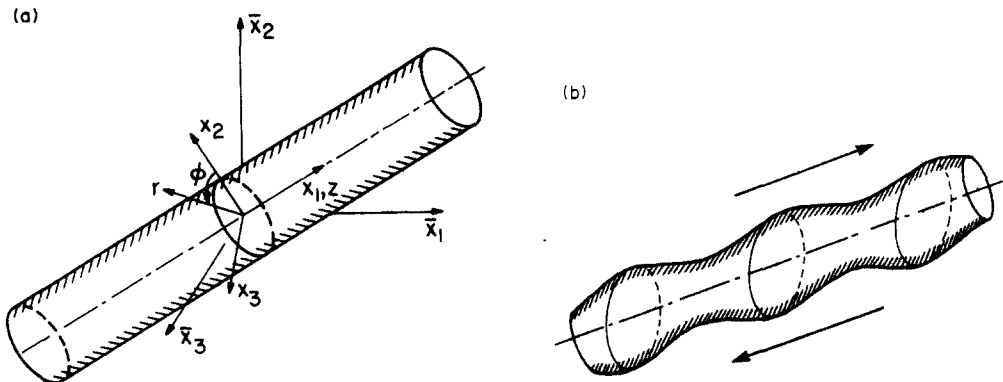


Figure 1. (a) Fluid filament with rotating frame fixed on its axis. (b) An initially axisymmetric disturbance convected by non-axisymmetric shear velocity on the drop surface.

We formally write a perturbation solution for the disturbance flow for this case as

$$\begin{aligned} v_{zm}^* &= v_{z0m}^*(r, z, \epsilon_1 \xi(\phi)) + \epsilon_1 v_{z1m}^*(r, z, \phi) + O(\epsilon_1^2), \\ v_{rm}^* &= v_{r0m}^*(r, z, \epsilon_1 \xi(\phi)) + \epsilon_1 v_{r1m}^*(r, z, \phi) + O(\epsilon_1^2), \\ v_{\phi m}^* &= \epsilon_1 v_{\phi 1m}^*(r, z, \phi) + O(\epsilon_1^2), \\ P_m^* &= P_{0m}^*(r, z, \epsilon_1 \xi(\phi)) + \epsilon_1 P_{1m}^*(r, z, \phi) + O(\epsilon_1^2), \end{aligned}$$

which reduces to the axisymmetric case in the limit  $\epsilon_1 \rightarrow 0$ .  $\epsilon_1 \xi(\phi)$  is a function which takes into account the asymmetry of the disturbance velocity field in the first-order terms. An analysis similar to that presented by Miakami *et al.* (1975) [for details the reader is referred to Khakhar (1986)] gives the result, to  $O(\epsilon)$ ,

$$\begin{aligned} \dot{a} + \epsilon \alpha \cos(kz + \epsilon_1 ka\beta) - \epsilon \alpha \sin(kz + \epsilon_1 ka\beta) (\dot{k}z + \epsilon_1 ka\dot{\beta}) \\ = -\frac{G_1}{2} \left[ a + \epsilon \alpha \cos(kz + \epsilon_1 ka\beta) \right] + \epsilon v_{r1}^* \\ + \left[ G_1 z + \frac{2}{(1+p)} (g_{12} \cos \phi + g_{13} \sin \phi) \right] \epsilon \alpha k \sin(kz + \epsilon_1 ka\beta), \end{aligned}$$

where the overdot represents  $d/dt$  and the stretching rate  $G_1 = \mathbf{L} : \mathbf{m}\mathbf{m}$  is a function of time and depends on the flow far away from the drop. The above condition is satisfied if the following relations hold:

$$\dot{a} = -\frac{G_1 a}{2} \quad [2]$$

for the drop radius;

$$\dot{k} = -G_1 k \quad [3]$$

for the wavenumber;

$$\dot{\alpha} = -\frac{G_1 \alpha}{2} + k[A_1 I_1(ka) + A_2 a I_1'(ka)] \quad [4]$$

for the amplitude; and

$$\epsilon_1 \dot{\beta} = -\frac{2}{(1+p)} (g_{12} \cos \phi + g_{13} \sin \phi) \quad [5]$$

for the phase shift. Equations [3] and [4] describe the rate of change of the wavenumber ( $k$ ) and amplitude of disturbances ( $\alpha$ ) growing on a fluid thread of mean radius  $a$ , stretching according to [2]. Equations [2]–[4] are similar in form to those of Mikami *et al.* (1975), thus to the order of approximation, our analysis shows that the asymmetry has a negligible effect on the rate of growth of small disturbances. The rate of stretching, however, varies with time as a result of the rotation of the filament and alters the dynamics of the breakup process. The rate of convection of disturbances is given by [5] which can be integrated independently, given the imposed flow, to give the total phase shift at any time. In what follows, we assume the phase shift to be small for all cases and subsequently calculate it as a check.

Defining a dimensionless wavenumber as

$$x = ka$$

and a characteristic time as  $S^{-1}$  with

$$S = (\mathbf{D} : \mathbf{D})^{1/2},$$

we find

$$\dot{x} = -\frac{1}{2} ex$$

and

$$\dot{a} = -\frac{1}{2}ea,$$

where  $e$  is the stretching efficiency defined as

$$e = \frac{G_1}{S} = \frac{\mathbf{D}:\bar{\mathbf{m}}\bar{\mathbf{m}}}{(\mathbf{D}:\mathbf{D})^{1/2}}$$

(Chella & Ottino 1985). On integration we find

$$x = x_0 \exp\left(-\frac{3}{2}\int_0^t e dt\right) \quad [6]$$

and

$$a = a_0 \left(\frac{x}{x_0}\right)^{1/3}, \quad [7]$$

where  $x_0$  and  $a_0$  are the initial wavenumber and radius, respectively. Substituting into the equation for amplitude, [4], we finally obtain

$$\frac{d \ln \alpha}{dt} = -\frac{e}{2} + \frac{x_0^{1/3}(1-x^2)}{2E x^{1/3}} \phi(x) - \frac{3}{2}e(p-1)\bar{\phi}(x), \quad [8]$$

where  $E = S\mu_e a_0/\sigma$  is the dimensionless strain rate and  $\phi(x)$  and  $\bar{\phi}(x)$  are known functions of the wavenumber and the viscosity ratio [see Mikami *et al.* (1975)].

#### BREAKUP OF LIQUID THREADS IN FLOWS WITH A NON-INCREASING STRAIN RATE

Here we discuss the growth of disturbances leading to the breakup of the filament for flows with a non-increasing strain rate, assuming that the equations for growth of disturbances derived for small amplitude and asymmetry remain valid even when both are of order 1. The behavior is qualitatively similar to the case of a filament in an axisymmetric extensional flow treated by Mikami *et al.* (1975), and we follow their arguments to derive criteria for breakup for the class of flows described above.

The equation for amplitude, [8], can be formally integrated to give

$$\ln \frac{\alpha}{\alpha_0} = \int_x^{x_0} \left[ \frac{x_0^{1/3}(1-x^2)}{3E x^{4/3}e} \phi(x) - \frac{(p-1)}{x} \bar{\phi}(x) \right] dx + \frac{1}{3} \ln \frac{x}{x_0}, \quad [9]$$

using [6] and [7]. From the above equation we can calculate the amplitude  $\alpha$  for a wavenumber  $x$  corresponding to the initial values  $x_0$  and  $\alpha_0$ . The typical behavior of the relative amplitude vs the wavenumber for the class of flows being considered is shown in figure 2a for a constant value of the dimensionless strain rate,  $E$ , and viscosity ratio,  $p$ . For sufficiently large initial wavenumbers, the relative amplitude decreases, then increases and finally decreases again. Disturbances with small initial wavenumbers are monotonically damped out. Concurrently the radius of the filament decreases with time.

Considering disturbances with a sufficiently large initial wavenumber, the wavenumber ( $x_m$ ) corresponding to the minimum in figure 2a can easily be found by putting

$$\frac{\partial}{\partial x} \left( \ln \frac{\alpha}{\alpha_0} \right) = 0, \quad [10a]$$

with the condition

$$\frac{\partial^2}{\partial x^2} \left( \ln \frac{\alpha}{\alpha_0} \right) > 0. \quad [10b]$$

On differentiating [9] we obtain

$$\frac{x_0^{1/3}(1-x_m^2)}{3E x_m^{4/3}e} \phi(x_m) - \frac{(p-1)}{x_m} \bar{\phi}(x_m) - \frac{1}{3x_m} = 0. \quad [11]$$

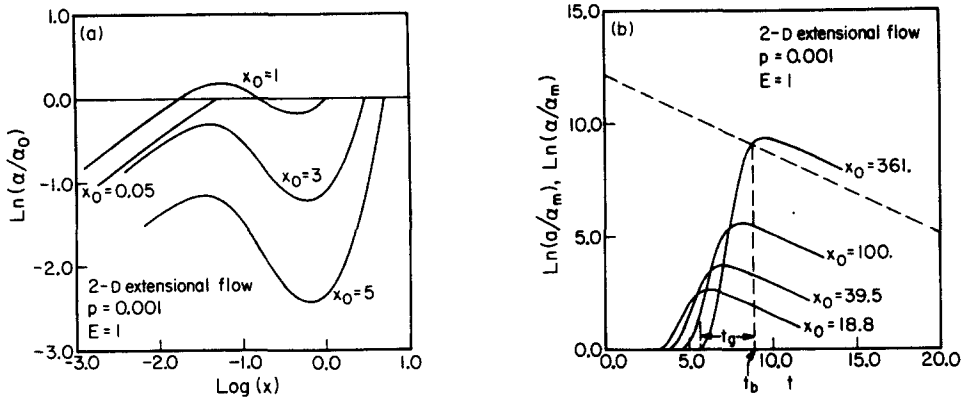


Figure 2. (a) Relative amplitude of the disturbance ( $\alpha/\alpha_0$ ) vs the dimensionless wavenumber ( $x$ ) for a filament in a hyperbolic extensional flow for a fixed value of the dimensionless strain rate ( $E$ ) and viscosity ratio ( $p$ ) for different initial wavenumbers ( $x_0$ ). (b) Magnification of disturbances ( $\alpha/\alpha_m$ ) vs time for a filament in a hyperbolic extensional flow for fixed value of the dimensionless strain rate ( $E$ ) and viscosity ratio ( $p$ ) and different initial wavenumbers ( $x_0$ ). The dashed line is the dimensionless mean radius ( $a/\alpha_m$ ) vs time for the same conditions. The first intersection of the plots of the magnification with the dashed line is the point of breakup of the filament. Note definitions for time for breakup ( $t_b$ ) and time for growth ( $t_g$ ) of the disturbances.

Condition [10b] must be checked by numerical differentiation to show that the extremum is a minimum.

Following Mikami *et al.* (1975), we define the magnification of disturbances as

$$M = \ln \frac{\alpha}{\alpha_m} \quad \text{for } \alpha > \alpha_m$$

$$0 \quad \text{for } \alpha < \alpha_m,$$

where  $\alpha_m$  is the amplitude of disturbances which are continuously generated at all wavelengths due to thermal and other fluctuations. The amplitude  $\alpha_m$  is thus taken to be the initial amplitude of all disturbances and corresponds to the minimum amplitude to which a disturbance can be damped out. Based on the above definition, the magnification of disturbances is given by

$$M = \int_x^{x_m} \left[ \frac{x_0^{1/3} (1-x^2)}{3E x^{4/3} e} \phi(x) - \frac{(p-1)}{x} \bar{\phi}(x) \right] dx + \frac{1}{3} \ln \frac{x}{x_m} \quad [12]$$

for  $x_m > x$  and 0 otherwise.

Mikami *et al.* (1975) showed that in the case of an axisymmetric extensional flow, for any given time there exists a disturbance with a wavenumber  $x_{opt}$  which has the maximum magnification. The arguments can easily be extended for the class of flows being studied here. The optimum wavenumber,  $x_{opt}$ , can be found by putting

$$\frac{\partial M}{\partial x_0} = 0 \quad [13a]$$

with the condition

$$\frac{\partial^2 M}{\partial x_0^2} < 0. \quad [13b]$$

Differentiating [12] with respect to  $x_0$ , keeping time constant, we find

$$\frac{\partial M}{\partial x_0} = \left[ f(x_m) - \frac{1}{3x_m} \right] \frac{\partial x_m}{\partial x_0} - \left[ f(x) - \frac{1}{3x} \right] \frac{\partial x}{\partial x_0} + \int_x^{x_0} \frac{\partial f}{\partial x_0} dx = 0,$$

where

$$f(x) = \frac{x_0^{1/3} (1-x^2)}{3E x^{4/3} e} \phi(x) - \frac{(p-1)}{x} \bar{\phi}(x).$$

Using [11] the above equation reduces to

$$\int_{x_{\text{opt}}}^{x_0} \frac{(1-x^2)}{x^{4/3}e} \phi(x) \left[ \frac{(x_0)_{\text{opt}}^{1/3}}{9Ee} + \frac{(x_0)_{\text{opt}}^{4/3}}{3E} \frac{\partial}{\partial x_0} \left( \frac{1}{e} \right) \right] dx + \left[ \frac{1}{3} - x_{\text{opt}} f(x_{\text{opt}}) \right] = 0. \quad [14]$$

Again the condition for the extremum to be a maximum, [13b], must be checked by numerical differentiation.

Finally, defining the point of breakup as the point when the amplitude of the disturbance is equal to the mean radius of the drop, we obtain

$$M = \ln \left[ \frac{a_0}{\alpha_m} \left( \frac{x_b}{x_0} \right)^{1/3} \right]$$

and, on substituting for magnification, we obtain

$$\ln \left( \frac{a_0}{\alpha_m x_{0b}^{1/3}} \right) = \int_{x_b}^{x_m} \left[ \frac{x_0^{1/3}}{3E} \frac{(1-x^2)}{x^{4/3}e} \phi(x) - \frac{(p-1)}{x} \bar{\phi}(x) \right] dx - \frac{1}{3} \ln x_m. \quad [15]$$

The above analysis of the dynamics of the growth of disturbances leading to the breakup of the thread may be visualized in physical terms as in figure 2b, in which we plot both the radius of the filament and the magnification ( $M$ ) of the disturbances with different initial wavenumbers ( $x_0$ ) vs time. The mean radius of the filament ( $a$ ) decreases with time due to the stretching of the filament. The wavenumber also decreases with time and depending on the initial wavenumber, the disturbances may grow or be damped out with time. If a disturbance is initially damped out, there is a time lag before the magnification increases from zero. At any given time there is a disturbance with a particular initial wavenumber which is magnified to the greatest extent. If the magnification of the disturbance at that time is equal to the mean radius of the thread, the thread is said to break.

We can now obtain the conditions at breakup, defined by  $x_b (=x_{\text{opt}})$ ,  $x_{0b} (=x_0)_{\text{opt}}$  and  $x_m$  from [11], [14] and [15], given  $E$ ,  $p$ ,  $a_0/\alpha_m$  and  $e = e(t, \bar{m}_0)$ , which depends on the imposed flow. The time for breakup,  $t_b$  (see figure 2b), can then be found from

$$\int_0^{t_b} e(t) dt = \ln \left( \frac{x_{0b}}{x_b} \right);$$

and the time for growth of disturbances,  $t_g$  (see figure 2b), from

$$\int_0^{t_g} e(t) dt = \ln \left( \frac{x_m}{x_b} \right).$$

Neglecting satellite drops, the radius of drop fragments produced on breakup can be estimated from the wavelength of the disturbance that causes breakup:

$$\frac{R_d}{a_0} = \left( \frac{3\pi}{2x_{0b}} \right)^{1/3},$$

as shown by Mikami *et al.* (1975).

It is clear from the above equations that in addition to the fluid properties ( $\sigma$ ,  $\mu_e$ ,  $\mu_l$ ), strain rate ( $S$ ) and type of flow, we require the initial conditions ( $a_0$ ,  $\bar{m}_0$ ) and the minimum amplitude of the disturbances ( $\alpha_m$ ) to make predictions using the above analysis. An estimate for  $\alpha_m$  may be obtained, assuming that the disturbances are due only to thermal fluctuations (Kuhn 1953), from

$$\alpha_m = \left( \frac{21kT}{8\pi^{3/2}\sigma} \right)^{1/2}, \quad [16]$$

where  $k$  is Boltzmann's constant and  $T$  is absolute temperature. The initial radius and orientation, however, cannot be as easily determined since in a real situation they are not independent variables. The initial conditions for this analysis correspond to the point when a stretched filament of fluid just becomes unstable with regard to surface disturbances. In general, the initial point would depend on the flow around the drop as well as the drop shape. From a theoretical viewpoint, a much more detailed analysis that takes into account the three-dimensional drop shape is required to predict the point of instability. Experimentally, Mikami *et al.* (1975) have suggested the following criterion to determine the initial point of the analysis:



“... not too long after application of the extensional flow, so that waves would not already have been amplified, and also not too soon after application of flow, so that one would have a uniform liquid thread.”

The initial conditions cannot be predicted from an analysis as above, and thus results of the analysis are given in terms of the initial conditions.

In the following sections we present calculations for a filament in a hyperbolic extensional flow and a simple shear flow, which are the only flows for which data on the dynamics of the breakup process are available at the moment of this writing.

### BREAKUP OF A FLUID THREAD IN A HYPERBOLIC EXTENSIONAL FLOW

In this case, in general, an arbitrarily oriented drop is quickly oriented along the direction of maximum stretching by the flow so that the initial orientation is unimportant, and the efficiency rapidly achieves its asymptotic value (Chella & Ottino 1985) given by

$$e = \frac{1}{\sqrt{2}}.$$

Since  $g_y = 0$ , the shear velocity along the surface disappears and

$$\beta = \beta = 0,$$

and the equations describing the growth of the disturbances reduce to those obtained by Mikami *et al.* (1975) for a filament in an axisymmetric extensional flow. Thus

$$\frac{x}{x_0} = \exp\left(-\frac{3}{2}et\right),$$

and on substituting into [11], [14] and [15] we obtain

$$\frac{x_{0b}^{1/3}}{eE} = \frac{3(p-1)\bar{\phi}(x_m) + 1}{(1-x_m^2)\phi(x_m)} x_m^{1/3}, \quad [17]$$

$$\frac{x_{0b}^{1/3}}{eE} \left[ \frac{(1-x_b^2)}{x_b^{4/3}} \phi(x_b) - \frac{1}{3} \int_{x_b}^{x_m} \frac{(1-x^2)}{x^{4/3}} \phi(x) dx \right] - 3(p-1)\bar{\phi}(x_b) - 1 = 0 \quad [18]$$

and

$$\ln\left(\frac{a_0}{\alpha_m x_{0b}^{1/3}}\right) = \int_{x_b}^{x_m} \left[ \frac{x_{0b}^{1/3}}{3eE} \frac{(1-x^2)}{x^{4/3}} \phi(x) - \frac{(p-1)\bar{\phi}(x)}{x} \right] dx - \frac{1}{3} \ln x_m. \quad [19]$$

Solution of the above set of non-linear equations could prove to be quite difficult and we propose the following indirect procedure which greatly simplifies the computation. We choose  $p$ ,  $(x_{0b}^{1/3}/Ee)$ ,  $x_m$ ,  $x_b$  and  $(a_0/\alpha_m x_{0b}^{1/3})$  as variables and carry out the following steps for a given  $p$ :

- (i) choose  $x_m$  in an appropriate range;
- (ii) calculate  $(x_{0b}^{1/3}/Ee)$  from [17];
- (iii) calculate  $x_b$  from [18] using  $x_m$  and the calculated value of  $(x_{0b}^{1/3}/Ee)$ ;
- (iv) calculate  $(a_0/\alpha_m x_{0b}^{1/3})$  from [19] using  $x_m$ ,  $x_b$  and  $(x_{0b}^{1/3}/Ee)$ .

In the above procedure, all the steps are explicit calculations except (iii) which requires an iterative calculation. From the results, since  $x_m$  is already specified, given either  $(a_0/\alpha_m)$  or  $E$  we can easily calculate the remaining quantities. Thus for each set of calculations for a given viscosity ratio and range of  $x_m$ , we can obtain graphs keeping either  $E$  or  $a_0/\alpha_m$  fixed. Mikami *et al.* (1975) presented their results as graphs keeping  $E$  fixed. For purposes of comparison with the case of a simple shear flow which we study next, we repeat some of the calculations carried out by Mikami *et al.* (1975); however, since we expect  $a_0/\alpha_m$  to be large and in a relatively small range, we present the results for different fixed values of  $a_0/\alpha_m$ . We also compare the theoretical predictions of the time for breakup ( $t_b$ ) with the data of Mikami *et al.* (1975), which was not done previously by the authors.

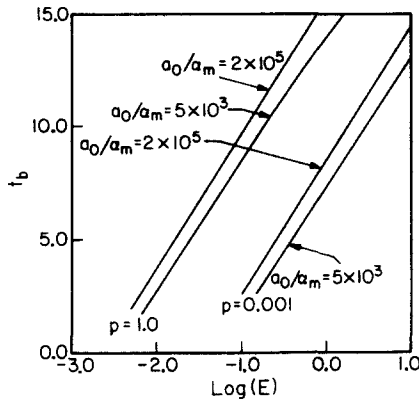


Figure 3. Dimensionless time for breakup ( $t_b$ ) vs the dimensionless strain rate ( $E$ ) for a filament in a hyperbolic extensional flow for fixed values of the viscosity ratio ( $p$ ) and dimensionless initial radius ( $a_0/\alpha_m$ ).

Figure 3 shows the time for breakup as a function of the dimensionless strain rate ( $E$ ) for different values of  $a_0/\alpha_m$  and the viscosity ratio. The time for breakup increases slowly with strain rate for fixed  $a_0/\alpha_m$ , and from the graph we find

$$t_b \propto v_1 \log(E);$$

the slope of the graph,  $v_1$ , being almost independent of the viscosity ratio and in the range 5.56–5.91 for the values of  $a_0/\alpha_m$  considered.

Figure 4 shows the radius of the drop fragments ( $R_d/a_0$ ) formed on breakup as a function of the dimensionless strain rate ( $E$ ) for the same conditions as above. There is a rapid decrease in the size of the drop fragments with increasing strain rate, and the graph indicates that

$$\frac{R_d}{a_0} \propto E^{v_2}$$

for fixed  $a_0/\alpha_m$ . Again the slope is almost independent of the viscosity ratio and takes on values in the range  $-0.83$  to  $-0.89$  for the range of  $a_0/\alpha_m$  considered. The number of drop fragments may be estimated from

$$N \propto \left(\frac{a_0}{R_d}\right)^3 \frac{l_0}{a_0},$$

where  $l_0$  is the initial length of the drop. Thus

$$N \propto E^{-3v_2}$$

for fixed  $a_0/\alpha_m$  and initial aspect ratio ( $a_0/l_0$ ).

Finally, we compare the predictions of the theory for the time for breakup with the data of Mikami *et al.* (1975) taken for drops in a hyperbolic extensional flow generated in a four-roll apparatus. Figure 5 shows the plot of the time for breakup vs the dimensionless strain rate for two viscosity ratios differing by an order of magnitude. The symbols represent the experimental data, while the lines are the predictions of the theory for the corresponding viscosity ratios and fixed values of  $a_0/\alpha_m$  chosen to span the experimentally obtained values of  $a_0$  with  $\alpha_m$  calculated from [16]. Unfortunately, the two sets of data do not cover a wide range of  $E$ . Figure 6 shows another way of comparing the data with the theoretical predictions. Here we plot  $t_b$  vs  $a_0/\alpha_m$  for the two viscosity ratios. Again the symbols represent the experimental data, with  $\alpha_m$  calculated using [16]. The lines are predictions of the theory for the corresponding viscosity ratios and fixed values of  $E$  spanning the range of experimentally obtained values of  $E$ . Considering that there are no adjustable parameters in the model, and the approximation involved, the agreement between the theory and experiment seems to be quite good. We next consider the breakup of a filament in a simple shear flow.

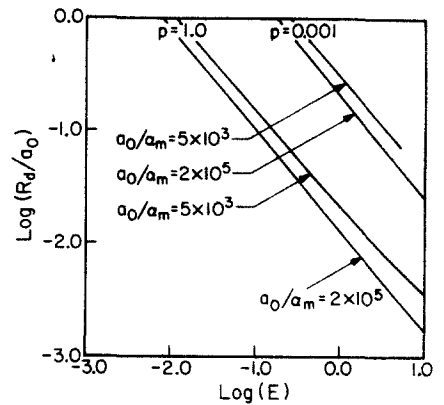


Figure 4. Dimensionless radius of spherical drop fragments formed on breakup ( $R_d/a_0$ ) vs the dimensionless strain rate ( $E$ ) for a filament in a hyperbolic extensional flow for fixed values of the viscosity ratio ( $p$ ) and dimensionless initial radius ( $a_0/\alpha_m$ ).

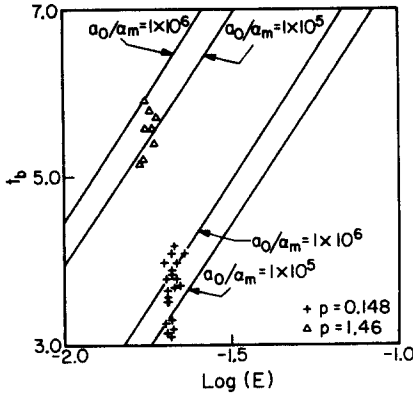


Figure 5. Dimensionless time for breakup ( $t_b$ ) vs the dimensionless strain rate ( $E$ ) for a filament in a hyperbolic extensional flow for fixed values of the viscosity ratio ( $p$ ) and dimensionless initial radius ( $a_0/\alpha_m$ ). Symbols represent the data of Mikami *et al.* (1975); lines are the predictions of the theory for the corresponding viscosity ratios ( $p$ ) and fixed values of  $a_0/\alpha_m$  spanning the experimentally obtained values of  $a_0$  with  $\alpha_m$  calculated from [16] (figure 6).

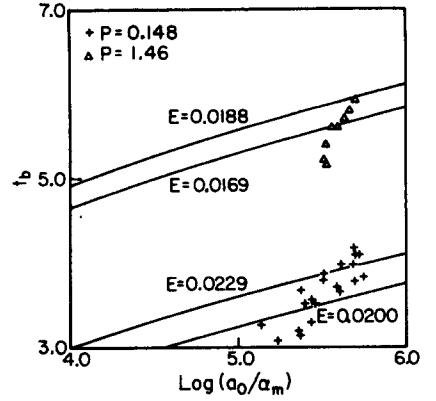


Figure 6. Dimensionless time for breakup ( $t_b$ ) vs the dimensionless initial radius ( $a_0/\alpha_m$ ) for a filament in a hyperbolic extensional flow for fixed values of the viscosity ratio ( $p$ ) and dimensionless strain rate ( $E$ ). Symbols represent the data of Mikami *et al.* (1975) with  $\alpha_m$  calculated from [16]; lines are the predictions of the theory for the corresponding viscosity ratios ( $p$ ) and fixed values of  $E$  spanning the experimentally obtained values (figure 5).

### BREAKUP OF A FLUID THREAD IN A SIMPLE SHEAR FLOW

According to our model, the stretching rate of the drop in a simple shear flow with shear rate  $\dot{\gamma}$  is given by

$$G_1 = \frac{\dot{\gamma} (\cot \theta_0 + \dot{\gamma} t)}{1 + (\cot \theta_0 + \dot{\gamma} t)^2},$$

where  $\theta_0$  is the initial angle between the streamlines and the axis of the thread. When the drop is almost aligned with the streamlines, as is expected in the case of a highly stretched drop, the stretching rate in dimensionless form is approximately given by

$$e = \frac{c}{1 + ct},$$

where  $c = 2 \tan \theta_0$ , and  $S = \dot{\gamma}/2$ . Integrating the equation for the wavenumber we obtain

$$\frac{x}{x_0} = (1 + ct)^{-3/2}$$

so that

$$e = c \left( \frac{x}{x_0} \right)^{2/3}.$$

The expression [5] describing the phase shift of the disturbance due to the non-axisymmetric shear flow reduces in this case to

$$\beta = -\frac{2\sqrt{2} (\cot^2 \theta_e - 1)}{1 + p (\cot^2 \theta_e + 1)} \cos \phi,$$

where we have put  $\epsilon_1 = 1$ . Again, since the drop is almost aligned with the streamlines, the above expression may be approximated by

$$\beta = -\frac{2\sqrt{2}}{1 + p} \cos \phi,$$

and on integration we obtain

$$\beta = -\frac{2\sqrt{2}}{1 + p} \cos \phi t_g,$$

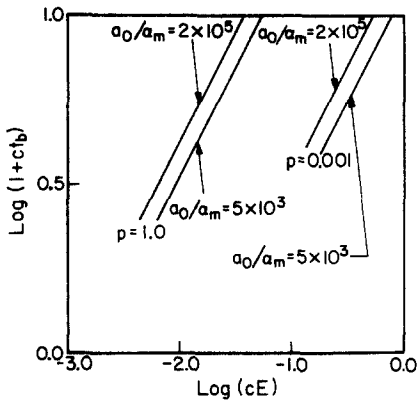


Figure 7. Normalized dimensionless time for breakup ( $ct_b$ ) vs the normalized dimensionless strain rate ( $cE$ ) for a filament in a simple shear flow for fixed values of the viscosity ratio ( $p$ ) and dimensionless initial radius ( $a_0/\alpha_m$ ).

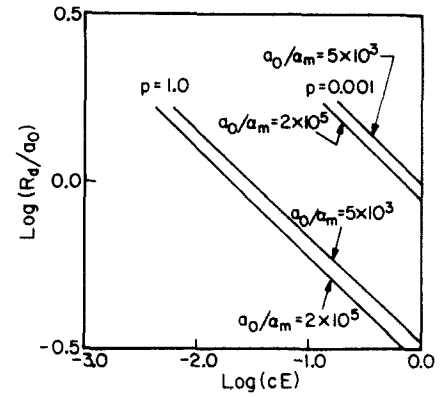


Figure 8. Dimensionless radius of spherical drop fragments formed on breakup ( $R_d/a_0$ ) vs the normalized dimensionless strain rate ( $cE$ ) for a filament in a simple shear flow for fixed values of the viscosity ratio ( $p$ ) and dimensionless initial radius ( $a_0/\alpha_m$ ).

where  $t_g$  is the time for growth of the disturbance (figure 2b). Thus the ratio of the maximum distance the disturbance is convected to the wavelength at the point of breakup is given by

$$\frac{\beta_{\max} a_b}{\lambda_b} = \frac{\sqrt{2}}{\pi} \frac{t_g x_b}{(1+p)}$$

The assumption of our analysis is validated if the above expression is small.

Substituting for the efficiency,  $e$ , into [11], [14] and [15] we obtain

$$\frac{x_{0b}}{cE} = \frac{3(p-1)\bar{\phi}(x_m) + 1}{(1-x_m^2)\phi(x_m)} x_m,$$

$$\frac{x_{0b}}{cE} \left[ \frac{(1-x_b^2)}{x_b} \phi(x_b) - \int_{x_b}^{x_m} \frac{(1-x^2)}{x^2} \phi(x) dx \right] - 3(p-1)\bar{\phi}(x_b) - 1 = 0$$

and

$$\ln\left(\frac{a_0}{\alpha_m x_{0b}^{1/3}}\right) = \int_{x_b}^{x_m} \left[ \frac{x_{0b}}{3cE} \frac{(1-x^2)}{x^2} \phi(x) - \frac{(p-1)\bar{\phi}(x)}{x} \right] dx - \frac{1}{3} \ln x_m.$$

The procedure we follow to solve the above set of equations is identical to that for the extensional flow earlier, except in this case the variables are  $p$ ,  $x_{0b}/cE$ ,  $x_b$ ,  $x_m$  and  $(a_0/\alpha_m x_{0b}^{1/3})$ . Also, in this case there is an additional unknown initial condition, the initial orientation of the filament which appears as a normalizing factor with the dimensionless time and strain rate. We present the results in terms of the initial conditions so that the time appears as  $ct$  and the strain rate as  $cE$ . As before, the calculations are for fixed  $a_0/\alpha_m$  and viscosity ratio.

Figure 7 shows the dimensionless time for breakup as a function of the dimensionless strain rate, both normalized by  $c$ , for the same conditions as figure 3 for the extensional flow. From the graph we find

$$(1+ct_b) \propto (cE)^{v_3}$$

for fixed  $a_0/\alpha_m$ , indicating a faster rate of increase for the time for breakup with increasing strain rate as compared to that for the extensional flow. The slope of the graph is almost independent of the viscosity ratio and  $a_0/\alpha_m$  with  $v_3 = 0.65$ .

Figure 8 shows the radius of the drop fragments on breakup ( $R_d/a_0$ ) vs the normalized dimensionless strain rate ( $cE$ ) for fixed  $a_0/\alpha_m$  and viscosity ratio, and should be compared to figure 4. The size of drop fragments decreases with increasing strain rate, and may be represented as

$$R_d/a_0 \propto (cE)^{v_4}$$

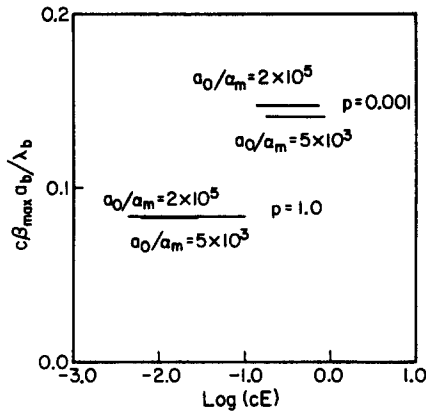


Figure 9. Normalized dimensionless maximum phase shift of the disturbance ( $c\beta_{\max} a_b/\lambda_b$ ) vs the normalized dimensionless strain rate ( $cE$ ) for a filament in a simple shear flow for fixed values of the viscosity ratio ( $p$ ) and dimensionless initial radius ( $a_0/\alpha_m$ ).

and the number of drops by

$$N \propto (cE)^{-3\nu_4}.$$

Again the slope of the graph is almost independent of the value of  $a_0/\alpha_m$  and the viscosity ratio and  $\nu_4 = -0.32$ . The results indicate that the rate of increase in the number of fragments with strain rate ( $E$ ) is slower than that obtained for the thread in the extensional flow. The drop fragments formed on breakup are also larger than those in hyperbolic extensional flow, for a given  $E$  and  $a_0$ , regardless of the value of  $c$ . Since  $c < 1$  and the radius of the drop fragments increases with decreasing  $c$  for a fixed value of  $E$ , a lower bound for the radius of the drop fragments may be obtained by assuming  $c = 1$ , leading to the above conclusion.

Finally, in figure 9 we plot the phase shift of the disturbance vs the strain rate for the same conditions as above. Since the time for growth ( $t_g$ ) can only be obtained in combination with the initial orientation, we plot  $c\beta_{\max} a_b/\lambda_b$  vs  $cE$ . The graph indicates that  $c\beta_{\max} a_b/\lambda_b$  is almost independent of the strain rate and takes on low values. However, since  $c$  is also small, the phase shift takes on larger values, and to check the validity of the assumption of small asymmetry we need to know the initial orientation. Thus, if  $c$  is not too small the assumption may be justified.

We also compare the theory with some experimental data of Grace (1971) in which the time for breakup, length at breakup and the number of drop fragments formed were recorded for drops in simple shear flow for strain rates above the critical strain rate. The comparison in this case is difficult since the experimentally measured quantities are different from the variables that appear in the analysis. The data are presented in terms of the following dimensionless quantities: ( $t_b^* \sigma/2\mu_e d$ ) is the dimensionless time for breakup, the time measured from the start of the experiment at which the drop is spherical, and  $d$  is the radius of the initially spherical drop; ( $l_b/2d$ ) is the dimensionless length at breakup; and ( $E^*/E_b^*$ ) is the ratio of the initial dimensionless strain rate to the dimensionless strain rate at breakup, where

$$E^* = \frac{\dot{\gamma} \mu_e d (19p + 16)}{\sigma (16p + 16)}.$$

No information is available about the initial conditions required for the theoretical analysis so that direct comparison to the data is impossible. Our approach here is to circumvent the requirement for the unknown quantities by combining variables so that the unknown quantities cancel out.

The initial point of the theoretical model is a filament of radius  $a_0$  that is just unstable to disturbances. If the time required to deform an initially spherical drop into a filament of radius  $a_0$  is neglected then

$$\frac{t_b^* \sigma}{2d\mu_e} = \frac{ct_b a_0}{cE 2d}.$$

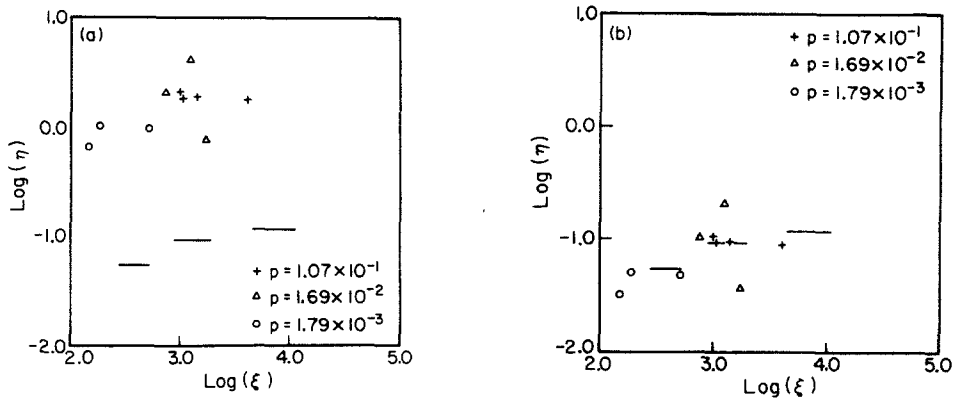


Figure 10 (a, b).  $\eta$  vs  $\xi$  (see the text for definitions) for a filament in a simple shear flow for fixed viscosity ratios ( $p$ ). Symbols represent the data of Grace (1971); lines are the predictions of theory for the corresponding viscosity ratios and fixed values of the dimensionless initial radius ( $a_0/\alpha_m = 3 \times 10^4$  and  $(a_0/\alpha_m) = 1 \times 10^5$ ). The lines for the two values of  $(a_0/\alpha_m)$  overlap.

Approximating the drop to be a circular cylinder of radius  $a_b$  and length  $l_b$ , at the point of breakup we obtain

$$\frac{l_b}{2d} = \frac{2}{3} \left( \frac{d}{a_b} \right)^2 = \frac{2}{3} \left( \frac{d}{a_0} \right)^2 \left( \frac{x_0}{x_b} \right)^{2/3}$$

using [6]. On appropriately combining the above two expressions we define a new variable  $\xi$ ,

$$\xi := \left( \frac{t_b^* \sigma}{2d\mu_c} \right)^2 \left( \frac{l_b}{2d} \right) = \frac{1}{6} \left( \frac{ct_b}{cE} \right)^2 \left( \frac{x_0}{x_b} \right)^{2/3},$$

so that the unknown quantities  $(a_0/d)$  and  $c$  cancel out. Neglecting satellite drops, the number of drop fragments may be estimated as

$$N = \left( \frac{a_0}{R_d} \right)^3 \left( \frac{d}{a_0} \right)^3.$$

We define a second variable  $\eta$ ,

$$\eta := N \left( \frac{l_b}{2d} \right)^{-3/2} = \left( \frac{3}{2} \right)^{3/2} \left( \frac{a_0}{R_d} \right)^3 \left( \frac{x_b}{x_0} \right),$$

so that again the unknown quantity,  $a_0/d$ , cancels out. The above simplifications allow comparison with the experimental data, however, the initial radius  $(a_0/\alpha_m)$  is still required in the calculations, and we simply choose a reasonable range of values.

Figure 10a shows a graph of  $\xi$  vs  $\eta$ . The symbols represent the data of Grace (1971), while the lines are the theoretical predictions for the corresponding viscosity ratios and fixed values of  $a_0/\alpha_m$ . The lines for the two values of  $a_0/\alpha_m$  overlap in this case so that range of values chosen does not seem to play a significant role. Though the behavior is qualitatively similar, the  $\eta$  values are much higher than the theoretical predictions. This may be attributed to the fact that satellite drops are included in the count in the number of drop fragments in the experimental data. The size distributions of the drop fragments formed on breakup for a set of experiments for drops of viscosity ratio  $p = 3.99 \times 10^{-3}$  for increasing values of  $(E^*/E_g^*)$  recorded by Grace (1971) indicate that the largest drop fragments comprise about 5% of the total number of fragments. If this fact is taken into account, there is better agreement between theory and experiment (figure 10b).

## CONCLUSIONS

In the above analysis we have studied the breakup of a filament of fluid acted upon by a general shear flow by means of a simplified model, the main component of which is the dynamic interaction between the growth of disturbances and the stretching of the filament as a function of the system

parameters. In the development of the model we have neglected the effect of a non-circular cross section and the drop ends, as well as any bending of the drop axis. The error due to all the above approximations, however, decreases with increasing slenderness of the drop. We have also neglected the asymmetry of disturbances due to the non-axisymmetric velocity along the drop surface. The asymmetry is the largest for the case of a simple shear flow, and our calculations for this case indicate that the assumption may be justified if the normalizing factor,  $c$ , which depends on the initial orientation, is not too small.

The predictions of the model seem to agree reasonably well with data for the dynamics of breakup, which at present are available only for the cases of a hyperbolic extensional flow and a simple shear flow. In the former case, we reinforce the findings of Mikami *et al.* (1975) by showing that the model is capable of predicting the time for breakup in addition to the wavelength at breakup, as shown by Mikami *et al.* (1975). For a filament in a simple shear flow, the data is too sparse to make a firm judgement on the model, however, there seems to be qualitative agreement in this case as well. In both cases, the model predicts the effect of the viscosity ratio on the dynamics quite well.

In addition, the model is simple enough to do detailed calculations of the breakup dynamics over wide parameter ranges and different types of flows including time-dependent flows, as might be encountered by a drop in a mixer. The main disadvantage is that initial conditions ( $a_0$ ,  $\bar{m}_0$ ) are required, and such data are generally difficult to obtain. However, solving the exact problem, even numerically, is extremely difficult if not impossible (Rallison & Acrivos 1978).

*Acknowledgements*—The authors acknowledge the financial support of the National Science Foundation, in the form of a PYI award (CPE-8351096), and the Department of Energy (DE-FG02-85ER13333). Also, we would like to thank one of the reviewers for very helpful comments.

#### REFERENCES

- BENTLEY, B. J. 1985 Drop deformation and burst in two-dimensional flows. Ph.D. Thesis, California Institute of Technology, Pasadena, Calif.
- CHELLA, R. & OTTINO, J. M. 1985 Stretching in some classes of fluid motions and asymptotic mixing efficiencies as a measure of flow classification. *Archs ration. Mech. Analysis* **90**, 15–42.
- GRACE, H. P. 1971 Dispersion phenomena in high viscosity immiscible fluid systems and application of static mixers as dispersion devices in such systems. Presented at *Engng Fdn Res. Conf. on Mixing*, Andover, N.H. [Also published in *Chem. Engng Commun.* **14**, 225–277 (1982).]
- HINCH, E. J. & ACRIVOS, A. 1980 Long slender drops in simple shear flow. *J. Fluid Mech.* **98**, 305–328.
- KARAM, H. J. & BELLINGER, J. C. 1968 Deformation and breakup of liquid droplets in simple shear flow. *Ind. Engng Chem. Fundam.* **7**, 576–583.
- KHAKHAR, D. V. 1986 Fluid mechanics of mixing: dispersion and chaotic flows. Ph.D. Thesis, Univ. of Massachusetts, Amherst, Mass.
- KHAKHAR, D. V., CHELLA, R. & OTTINO, J. M. 1984 Stretching, chaotic motion, and breakup of elongated droplets in time-dependent flows. In *Advances in Rheology*, Vol. 2, *Fluids (Proceedings of the IXth International Congress of Rheology)* (Edited by MENA, B., GARCIA-REJON, A. & RANGEL-NAFAILE, C.). Universidad Autonoma de Mexico, Mexico.
- KHAKHAR, D. V. & OTTINO, J. M. 1986 Deformation and breakup of slender drops in linear flows. *J. Fluid Mech.* (to appear).
- KUHN, W. 1953 Spontane Aufteilung von Flüssigkeitszylindern in Klein Kugeln. *Kolloid Z.* **132**, 84–99.
- MIKAMI, T., COX, R. G. & MASON, R. G. 1975 Breakup of extending liquid threads. *Int. J. Multiphase Flow* **2**, 113–118.
- RALLISON, J. M. 1984 The deformation of small viscous drops in shear flows. *A. Rev. Fluid Mech.* **16**, 45–66.
- RALLISON, J. M. & ACRIVOS, A. 1978 A numerical study of the deformation and burst of a viscous drop in an extensional flow. *J. Fluid Mech.* **89**, 191–200.

- TAYLOR, G. I. 1934 The formation of emulsions in definable fields of flow. *Proc. R. Soc.* **A146**, 501–523.
- TOMOTIKA, S. 1936 Breakup of a drop of viscous liquid immersed in another viscous fluid which is extending at a uniform rate. *Proc. R. Soc.* **A153**, 302–318.
- TORZA, S., COX, R. G. & MASON, S. G. 1972 Particle motions in sheared suspensions. XXVII. Transient and steady deformation and burst of liquid drops. *J. Colloid Interface Sci.* **38**, 395–411.